Journal of Hyperbolic Differential Equations
Vol. 5, No. 2 (2008) 295–315

World Scientific
www.worldscientific.com

LAX SHOCKS IN MIXED-TYPE SYSTEMS OF CONSERVATION LAWS

ALEXEI A. MAILYBAEV

Institute of Mechanics
Moscow State Lomonosov University
Michurinsky pr. 1, 119192 Moscow, Russia
mailybaev@imec.msu.ru

DAN MARCHESIN

Instituto Nacional de Matemática Pura e Aplicada – IMPA
Estrada Dona Castorina, 110
22460-320 Rio de Janeiro RJ, Brazil
marchesi@impa.br

Received 25 Jan. 2007
Accepted 18 Feb. 2008

Communicated by Gui-Qiang Chen

Abstract. Small amplitude shocks involving a state with complex characteristic speeds arise in mixed-type systems of two or more conservation laws. We study such shocks in detail in the generic case, when they appear near the codimension-1 elliptic boundary. Then we classify all exceptional codimension-2 states on smooth parts of the elliptic boundary. Asymptotic formulae describing shock curves near regular and exceptional states are derived. The type of singularity at the exceptional point depends on the second and third derivatives of the flux function. The main application is understanding the structure of small amplitude Riemann solutions where one of the initial states lies in the elliptic region.

Keywords: Mixed-type system of conservation laws; shock wave; elliptic region; Riemann problem; singularity; exceptional point.

Mathematics Subject Classification 2000: 35M10, 76L05

1. Introduction

Shock waves are responsible for the mathematical interest of the theory of nonlinear conservation laws. When only strictly hyperbolic states (i.e. all characteristic speeds are real and distinct) are involved and under additional technical hypotheses, shock waves are usually extremely stable and well behaved, see e.g. [25]. A number of models studied recently contain elliptic regions, see [3–5,12,15,22,23] and the review in [19]. In these models, some stable shock waves typically contain points near

the boundary of the elliptic region. Hugoniot curves near regular points of elliptic boundaries were studied in [12] for a specific system with nonhomogeneous quadratic flux, and in [14] for equations reduced to normal form. Related Riemann solutions were discussed in [5, 7, 12, 21].

In this work, we study shock curves for systems of m conservation laws in the neighborhood of the elliptic boundary, which is defined as the surface where two characteristic speeds coincide. The local structure of shock waves is described near regular and exceptional states of the elliptic boundary. Here the exceptional states are the points on the elliptic boundary where the eigenvector is tangent to the boundary. Exceptional points typically exist on the boundaries of elliptic regions, for example, in systems with nonhomogeneous quadratic fluxes. The structure of shock wave is very special near exceptional points. Note that the structure of rarefaction waves is also singular near exceptional points, as shown in [16].

In this paper, the classification of exceptional points according to the local behavior of shock curves is given. Explicit formulae providing qualitative and quantitative description of shock curve singularities are derived. These formulae use eigenvectors and associated vectors of coincident characteristic speeds as well as the derivatives up to third order of the flux function at the point of the elliptic boundary. The importance of the third derivative of the flux function is remarkable at exceptional states. As a result, the quadratic approximation of the flux function is insufficient for local analysis of shock curves near such states.

Our method is based on the Liapunov–Schmidt reduction of Rankine–Hugoniot equation written in a specific ("blow-up") coordinate system. This coordinate system is similar to that used for constructing the wave manifold in [13]. The Lax conditions for shocks are checked by using bifurcation theory of multiple eigenvalues [24].

The paper is organized as follows. Section 2 contains general information on shock waves. Section 3 studies shock waves with states near regular points of the elliptic boundary. In Sec. 4, a similar analysis is carried out near exceptional points of the elliptic boundary. Section 5 gives a numerical example of a Riemann solution with one initial state inside the elliptic region. The paper ends with a short discussion.

2. Shock Waves in Conservation Laws

Let us consider a system of m conservation laws in one space dimension x:

$$\frac{\partial U}{\partial t} + \frac{\partial F(U)}{\partial x} = 0, \tag{2.1}$$

where $U(x,t) \in \mathbb{R}^m$ is a vector of conserved quantities, and $F \in \mathbb{R}^m$ is a flux function smoothly dependent on U. Let $A(U) = \partial F/\partial U$ be the $m \times m$ Jacobian matrix of the flux function $F(U)$. Then the system is (strictly) hyperbolic at U if all the eigenvalues of the matrix $A(U)$ are real (and distinct). The elliptic region consists of the points U where the matrix $A(U)$ possesses complex eigenvalues.

In the region of strict hyperbolicity, we list the eigenvalues of $A(U)$ (characteristic speeds) in increasing order as $\lambda_1(U) < \lambda_2(U) < \cdots < \lambda_m(U)$.

A shock wave is a discontinuity in a (weak) solution of system (2.1) at $x = x_s(t)$. It consists of a left state $U_- = \lim_{x \to x_s(t)-0} U(x,t)$ and a right state $U_+ = \lim_{x \to x_s(t)+0} U(x,t)$; the shock speed is $\sigma = dx_s/dt$. The left and right states and the speed of the shock must satisfy the Rankine–Hugoniot condition

$$F(U_+) - F(U_-) = \sigma(U_+ - U_-), \tag{2.2}$$

following from the requirement that the shock is a weak solution of (2.1) [25]. We will consider as admissible the shocks satisfying the extended Lax conditions

$$\begin{aligned}
&1\text{-shock: } \sigma < \operatorname{Re}\lambda_1(U_-), \quad \operatorname{Re}\lambda_1(U_+) < \sigma < \operatorname{Re}\lambda_2(U_+);\\
&\qquad\vdots\\
&k\text{-shock: } \operatorname{Re}\lambda_{k-1}(U_-) < \sigma < \operatorname{Re}\lambda_k(U_-), \quad \operatorname{Re}\lambda_k(U_+) < \sigma < \operatorname{Re}\lambda_{k+1}(U_+);\\
&\qquad\vdots\\
&m\text{-shock: } \operatorname{Re}\lambda_{m-1}(U_-) < \sigma < \operatorname{Re}\lambda_m(U_-), \quad \operatorname{Re}\lambda_m(U_+) < \sigma,
\end{aligned} \tag{2.3}$$

where the integer k denotes shock family number. For states $U_\pm$ in the hyperbolic region (when the characteristic speeds are real), inequalities (2.3) are the classical Lax conditions. They are sufficient for stability of small shocks under some additional technical conditions, see e.g. [25]. When at least one of the states $U_\pm$ lies in the elliptic region (when the characteristic speeds are complex), inequalities (2.3) extend the Lax condition for the case of conservation laws with vanishing diffusion of the form

$$\frac{\partial U}{\partial t} + \frac{\partial F(U)}{\partial x} = \epsilon \frac{\partial^2 U}{\partial x^2}, \quad \epsilon \to +0. \tag{2.4}$$

Under conditions (2.3), if a traveling wave in (2.4) exists for a shock wave with certain left and right states $U_\pm$, then the traveling wave generically exists for shocks under small perturbations of left and right states satisfying (2.2). Examples show that inequalities (2.3) are not sufficient for the stability of the traveling wave [6,10]. In this paper, we use extended Lax admissibility conditions in a formal way without checking stability.

For fixed U_-, Eq. (2.2) determines a set of curves in state space U_+; we will call them the Hugoniot curve. It is known that, for U_- lying in the region of strict hyperbolicity, there are m Hugoniot curves passing through U_-; each curve is tangent to the eigenvector of the matrix $A(U_-)$ at U_-.

3. Shock Curves Near the Elliptic Boundary

In this paper, we study small-amplitude shocks with states near the boundary of the elliptic region. Consider a point U_0 on the elliptic boundary. In the generic case, two

real eigenvalues (characteristic speeds) λ_k and λ_{k+1} coincide at U_0 forming a 2×2 Jordan block [1]. We denote $A_0 = A(U_0)$ and $\sigma_0 = \lambda_k(U_0) = \lambda_{k+1}(U_0)$. Then there is a real eigenvector r_0 and a generalized eigenvector (associated vector) r_1 satisfying the Jordan chain equations

$$A_0 r_0 = \sigma_0 r_0, \quad A_0 r_1 = \sigma_0 r_1 + r_0. \tag{3.1}$$

The generalized eigenvector r_1 can be chosen to be orthogonal to r_0, so we assume that

$$r_0 \cdot r_0 = 1, \quad r_0 \cdot r_1 = 0, \tag{3.2}$$

where the dot denotes the standard inner product in $\mathbb{R}^m$ (generally $\|r_1\| \neq 1$). In addition to the (right) vectors r_0, r_1, we define the left eigenvector l_0 and generalized eigenvector l_1 as (both l_0 and l_1 are row-vectors)

$$l_0 A_0 = \sigma_0 l_0, \quad l_1 A_0 = \sigma_0 l_1 + l_0, \tag{3.3}$$

$$l_0 r_1 = 1, \qquad l_1 r_1 = 0. \tag{3.4}$$

The normalization conditions (3.4) define uniquely l_0 and l_1 for given r_0, r_1. Furthermore, these vectors satisfy the relations (see e.g. [24])

$$l_0 r_0 = 0, \quad l_1 r_0 = l_0 r_1 = 1. \tag{3.5}$$

For small shocks near the elliptic boundary, we can write

$$U_- = U_0 + u, \quad U_+ = U_0 + u + \xi e, \quad \sigma = \sigma_0 + \varepsilon. \tag{3.6}$$

Here $u \in \mathbb{R}^m$, $\xi \in \mathbb{R}$, and $\varepsilon \in \mathbb{R}$ are small, and the direction vector $e \in \mathbb{R}^m$ has unit norm $\|e\| = 1$. Here we use coordinates similar to the coordinates on the wave manifold introduced in [13]. Note that the coordinates with e and ξ changed by $-e$ and $-\xi$ are identical. For $U_- = U_+$ one has $\xi = 0$ and arbitrary e (this is the essence of the "blow-up" procedure used in [13]). As we will see below, these coordinates facilitate the analysis.

By using (3.6), the Rankine–Hugoniot conditions (2.2) can be rewritten as

$$\Phi(\xi, e, \varepsilon, u) \equiv \frac{F(U_0 + u + \xi e) - F(U_0 + u)}{\xi} - (\sigma_0 + \varepsilon) e = 0. \tag{3.7}$$

It is easy to see that the function $\Phi(\xi, e, \varepsilon, u)$ is smooth with respect to all variables. At $u = 0$ and $\xi = \varepsilon = 0$, Eq. (3.7) takes the form

$$A_0 e - \sigma_0 e = 0, \tag{3.8}$$

which implies that $e = r_0$ (the sign of r_0 is irrelevant due to the equivalence $(e, \xi) \leftrightarrow (-e, -\xi)$ mentioned above). Hence, we must look for a solution of the equation $\Phi(\xi, e, \varepsilon, u) = 0$ in the neighborhood of the point $(0, r_0, 0, 0)$.

3.1. *Asymptotic relation for the Hugoniot curve*

Let us introduce the vectors $n, q \in \mathbb{R}^m$ as

$$n \cdot a \equiv l_0 d^2F(a, r_0), \quad q \cdot a \equiv \frac{1}{2}\, l_1 d^2F(a, r_0) + \frac{1}{2}\, l_0 d^2F(a, r_1). \tag{3.9}$$

Here $d^2F(a, b)$ denotes the second-order derivative of the flux function at U_0:

$$d^2F(a, b) = \sum_{i,j=1}^{m} \frac{\partial^2 F}{\partial U_i \partial U_j}\Big|_{U=U_0} a_i b_j, \quad a, b \in \mathbb{R}^m, \tag{3.10}$$

so that

$$F(U_0 + \Delta U) = F(U_0) + A_0 \Delta U + \frac{1}{2}\, d^2F(\Delta U, \Delta U) + o(\|\Delta U\|^2). \tag{3.11}$$

Theorem 3.1. *Assume that at the elliptic boundary point U_0 the nondegeneracy condition*

$$n \cdot r_0 \neq 0 \tag{3.12}$$

is satisfied, then Eq. (3.7) *has a unique solution $\xi(\varepsilon, u)$, $e(\varepsilon, u)$ in the neighborhood of $(\xi, e, \varepsilon, u) = (0, r_0, 0, 0)$. It has the form*

$$\xi(\varepsilon, u) = 2\, \frac{\varepsilon^2 - n \cdot u}{n \cdot r_0} + o(\varepsilon^2, \|u\|), \tag{3.13}$$

$$e(\varepsilon, u) = r_0 + r_1 \varepsilon + e_u u + o(\varepsilon, \|u\|), \tag{3.14}$$

where

$$e_u u = G\left(\frac{n \cdot u}{n \cdot r_0}\, d^2F(r_0, r_0) - d^2F(u, r_0)\right), \quad G = (A_0 - \sigma_0 I + r_1 r_0^T)^{-1}. \tag{3.15}$$

Proof. Let us consider the Taylor expansion of the function Φ at the point $(\xi, e, \varepsilon, u) = (0, r_0, 0, 0)$. As it was shown above, the function Φ vanishes at $(0, r_0, 0, 0)$ (expression (3.7) is reduced to (3.8)). Using expression (3.11) in (3.7) yields for the first and second order terms

$$\begin{aligned}
\Phi(\xi, e, \varepsilon, u) = {} & \frac{1}{2}\, d^2F(r_0, r_0)\, \xi + (A_0 - \sigma_0 I)\, h - r_0\, \varepsilon + d^2F(u, r_0) \\
& + \frac{1}{6}\, d^3F(r_0, r_0, r_0)\, \xi^2 + \frac{1}{2}\, d^3F(u, r_0, r_0)\, \xi + d^2F(h, r_0)\, \xi + d^2F(u, h) \\
& + \frac{1}{2}\, d^3F(u, u, r_0) - h\varepsilon + \cdots \\
= {} & 0,
\end{aligned} \tag{3.16}$$

where $h = e - r_0$, I is the identity matrix, and $d^3F(a, b, c)$ is the third derivative of the flux function defined in a way analogous to the second derivative in (3.10). For small ξ, h, ε and u, Eq. (3.7) with $\|e\| = 1$ has a unique solution $\xi(\varepsilon, u)$, $e(\varepsilon, u)$ if the $m \times (m + 1)$ Jacobian matrix $\left[\frac{1}{2} d^2F(r_0, r_0),\ A_0 - \sigma_0 I\right]$ has full rank. Since the

left null-space of $A_0 - \sigma_0 I$ is one-dimensional and it is defined by the left eigenvector l_0, this condition is equivalent to

$$l_0 d^2 F(r_0, r_0) = n \cdot r_0 \neq 0. \tag{3.17}$$

This inequality is satisfied by the assumption (3.12) of the theorem.

Multiplying (3.16) by l_0 from the left, and using (3.3), (3.5), (3.9), we obtain

$$l_0 \Phi(\xi, e, \varepsilon, u) = \frac{n \cdot r_0}{2}\, \xi + n \cdot u + o(\xi, \|h\|, \varepsilon, \|u\|) = 0. \tag{3.18}$$

Hence, we find $\xi(\varepsilon, u)$ up to first order terms as

$$\xi(\varepsilon, u) = -\frac{2n \cdot u}{n \cdot r_0} + o(\varepsilon, \|u\|). \tag{3.19}$$

In first order approximation, we have $r_0 \cdot h = 0$ (recall that $e = r_0 + h$ is the unit norm vector). In order to find h, it is convenient to add $(r_0 \cdot h) r_1 = 0$ to the expression (3.16). Then, by using (3.19) and keeping only the first order terms, we write the equation $\Phi = 0$ as

$$(A_0 - \sigma_0 I + r_1 r_0^T)\, h - r_0\, \varepsilon + d^2 F(u, r_0) - \frac{n \cdot u}{n \cdot r_0}\, d^2 F(r_0, r_0) = 0. \tag{3.20}$$

The matrix $A_0 - \sigma_0 I + r_1 r_0^T$ is nonsingular ($r_1 r_0^T$ is the diadic product matrix). The inverse matrix $G = (A_0 - \sigma_0 I + r_1 r_0^T)^{-1}$ defined in (3.15) satisfies the relations

$$G r_0 = r_1, \quad G r_1 = r_0, \quad l_0 G = l_1, \quad r_0^T G = l_0, \tag{3.21}$$

which can be verified by using (3.1)–(3.5). Then one solves Eq. (3.20) in the form (3.14), (3.15).

Now let us evaluate the second derivative of (3.16) with respect to ε as a composite function (i.e. with $\xi = \xi(\varepsilon, u)$ and $e = e(\varepsilon, u)$). At $(\varepsilon, u) = (0, 0)$, the following equalities hold: $\xi = 0$, $e = r_0$ and $\xi_\varepsilon = 0$, $e_\varepsilon = h_\varepsilon = r_1$. Thus, we obtain

$$\Phi_{\varepsilon\varepsilon} = \frac{1}{2}\, d^2 F(r_0, r_0)\, \xi_{\varepsilon\varepsilon} + (A_0 - \sigma_0 I)\, h_{\varepsilon\varepsilon} - 2 r_1 = 0 \tag{3.22}$$

(the subscripts ε denote derivatives). Multiplying by l_0 from the left and using (3.3), (3.4), we find $\xi_{\varepsilon\varepsilon} = 4/(n \cdot r_0)$. This provides the coefficient of the ε^2 term in (3.13). □

3.2. *Singularities of Hugoniot curves*

Using expressions (3.13) and (3.14) of Theorem 3.1 in (3.6), we obtain the following asymptotic relations for shock states and speed

$$U_- = U_0 + u, \quad U_+ = U_0 + u + 2\, \frac{\varepsilon^2 - n \cdot u}{n \cdot r_0}\, (r_0 + \varepsilon r_1), \quad \sigma = \sigma_0 + \varepsilon. \tag{3.23}$$

Here we kept only the essential lowest order terms in the expression for U_+. The term $e_u u$ is dropped in the parenthesis in (3.23). As we will see below, the geometry

of the shock curve is described by ε in the interval $\varepsilon \lesssim \sqrt{\|u\|}$, so $e_u u \sim \varepsilon^2$ is a higher order correction term.

The vector n defined in (3.9) is normal to the elliptic boundary at U_0, pointing into the hyperbolic region, see e.g. [24]. Thus, the nondegeneracy condition (3.12) implies that the eigenvector r_0 is transversal to the elliptic boundary at U_0.

Assuming that u is small and fixed (the left state U_- is fixed near the elliptic boundary), we have three different forms for the Hugoniot curve in U_+ state as shown in Fig. 1. The three cases are distinguished by the sign of the quantity $n \cdot u$. If $u = 0$, then the Hugoniot curve has a cusp at the point $U_- = U_0$. This corresponds to a left state U_- lying exactly on the elliptic boundary. The cusp consists of two curves that are tangent to the eigenvector r_0 and lie in the hyperbolic region. Asymptotically, the Hugoniot curve lies in the plane spanned by the vectors r_0 and r_1.

If $n \cdot u > 0$, then the left state $U_- = U_0 + u$ belongs to the hyperbolic region, and the Hugoniot curve forms a loop with self-intersection at $U_+ = U_-$. The self-intersection point corresponds to the shock speeds $\sigma = \sigma_0 \pm \sqrt{n \cdot u}$. Asymptotically, the elliptic boundary crosses the loop at the middle. This means that there is a line segment parallel to the eigenvector r_0 with one end at $U_- = U_0 + u$ and opposite end at $U_+^* = U_0 + u - 2\,\frac{n \cdot u}{n \cdot r_0} r_0$ (the point corresponding to $\varepsilon = 0$), which intersects the elliptic boundary at the middle, see Fig. 1(b). At the point U_+^*, the vector r_1 is tangent to the Hugoniot curve. As $U_- \to U_0$, the loop of the Hugoniot curve shrinks forming the cusp singularity in Fig. 1(a). It is easy to see from expressions (3.23) that the angle at the self-intersection point tends to zero asymptotically as $2\|r_1\|\sqrt{n \cdot u}$. Recall that the tangent vectors to the Hugoniot curve at the self-intersection point $U_- = U_+$ are the eigenvectors of the matrix $A(U_-)$. These two eigenvectors merge as U_- approaches the elliptic boundary. Note that the loop in Fig. 1(b) was recognized in [14] by using theory of normal forms.

If $n \cdot u < 0$, then the left state $U_- = U_0 + u$ belongs to the elliptic region, and the Hugoniot curve does not pass through U_-, so it does not have self-intersection

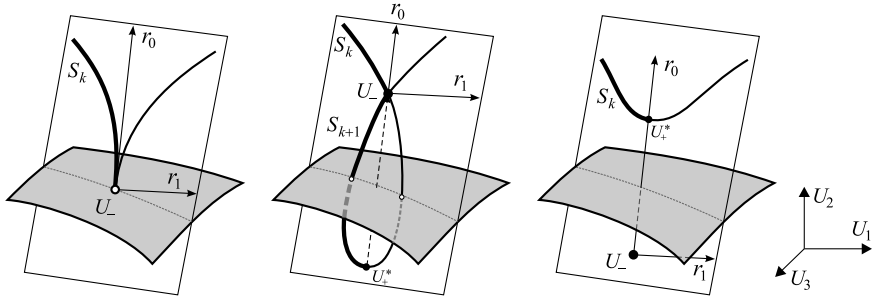

Fig. 1. Hugoniot curves for fixed left states U_- on or near the elliptic boundary. The elliptic region lies below the gray surface.

points. The whole curve lies in the hyperbolic region. Asymptotically, the point U_+^* of the curve nearest to the elliptic boundary corresponds to $\varepsilon = 0$. The segment between U_- and U_+^* is parallel to r_0 and asymptotically intersects the elliptic boundary at the middle; it is also orthogonal to the Hugoniot curve at U_+^*, see Fig. 1(c). We see that, for small shocks involving a state inside the elliptic region, the other state is always in the hyperbolic region.

3.3. *Admissible shocks near the elliptic boundary*

Let us check the Lax conditions (2.3) for different points of the Hugoniot curve. In the case when A_0 has double eigenvalue σ_0 with 2×2 Jordan block, the asymptotic expression for the eigenvalues of the perturbed matrix $A_0 + B$ is given by [24]

$$\lambda_{k,k+1} = \sigma_0 \pm \sqrt{l_0 B r_0 + o(\|B\|)} + \frac{1}{2}\,(l_1 B r_0 + l_0 B r_1) + o(\|B\|). \tag{3.24}$$

Hereafter, λ_k corresponds to the minus sign, and λ_{k+1} corresponds to the plus sign of the square root. Taking $B = A(U) - A_0$ (so that $A_0 + B = A(U) = dF/dU$) evaluated at $U = U_0 + \Delta U$, we have

$$B\,a = d^2F(\Delta U, a) + \frac{1}{2}\,d^3F(\Delta U, \Delta U, a) + o(\|\Delta U\|^2), \quad a \in \mathbb{R}^m. \tag{3.25}$$

Using the vectors n and q defined in (3.9), we obtain

$$\lambda_{k,k+1}(U_0 + \Delta U) = \sigma_0 \pm \sqrt{n \cdot \Delta U + o(\|\Delta U\|)} + q \cdot \Delta U + o(\|\Delta U\|). \tag{3.26}$$

For U_- and U_+ given by expressions (3.23), we find the asymptotic relations

$$\lambda_{k,k+1}(U_-) = \sigma_0 \pm \sqrt{n \cdot u}, \quad \lambda_{k,k+1}(U_+) = \sigma_0 \pm \sqrt{2\varepsilon^2 - n \cdot u}. \tag{3.27}$$

In these expressions, we kept only the lowest order (square root) terms.

First, consider the left states U_- in the hyperbolic region ($n \cdot u > 0$). If $|\varepsilon| > \sqrt{(n \cdot u)/2}$, then the second square root in (3.27) is real, so U_+ belongs to the hyperbolic region. Then, by using (3.27) in (2.3), we find that the admissible k-shocks correspond to $\varepsilon < -\sqrt{n \cdot u}$, and $(k+1)$-shocks correspond to $\sqrt{(n \cdot u)/2} < \varepsilon < \sqrt{n \cdot u}$. For U_+ in the elliptic region ($|\varepsilon| < \sqrt{(n \cdot u)/2}$), the square root term in the second expression in (3.27) is purely imaginary (the expression inside the square root is negative). Then $\operatorname{Re}\lambda_k = \operatorname{Re}\lambda_{k+1} = \sigma_0 + o(\|u\|^{1/2})$, and we have $(k+1)$-shocks for $\varepsilon > o(\|u\|^{1/2})$. Thus, right states of $(k+1)$-shocks correspond to the segment between the point U_- and the opposite point of the loop U_+^* in Fig. 1(b). Therefore, we found that the shocks satisfying the extended Lax conditions are given by

$$\begin{gathered} k\text{-shock: } \varepsilon < -\sqrt{n \cdot u}, \\ (k+1)\text{-shock: } 0 < \varepsilon < \sqrt{n \cdot u}, \end{gathered} \tag{3.28}$$

with the terms of order $\|u\|$ neglected. These shocks are represented by thick segments S_k and S_{k+1} in Fig. 1(b). If we interchange the left and right states U_- and U_+, the other two (thin) segments correspond to admissible shocks.

Now consider the left states U_- in the elliptic region ($n \cdot u < 0$). In this case $\operatorname{Re}\lambda_k(U_-) = \operatorname{Re}\lambda_{k+1}(U_-) = \sigma_0 + o(\|u\|^{1/2})$, so only k-shocks are possible. By checking conditions (2.3), one finds with the accuracy $o(\|u\|^{1/2})$:

$$k\text{-shock: } \varepsilon < 0. \tag{3.29}$$

These shocks are represented by the thick segment S_k in Fig. 1(c). If we interchange the left and right states U_- and U_+, the other (thin) segment corresponds to admissible $(k+1)$-shocks.

A similar analysis for the left states U_- at the elliptic boundary ($u = 0$) yields existence of k-shocks only. These shocks are given by condition (3.29) (which is exact), and are represented by the thick segment S_k in Fig. 1(a). The other (thin) segment of the Hugoniot curve in Fig. 1(a) corresponds to $(k+1)$-shocks from U_+ to U_- (with the left and right states interchanged).

4. Exceptional Points of Elliptic Boundary

Let us consider a point of the elliptic boundary U_0, where the nondegeneracy condition (3.12) is violated, i.e. the eigenvector r_0 is tangent to the elliptic boundary:

$$n \cdot r_0 = 0. \tag{4.1}$$

Such a point was called exceptional in [16]. Generically, a set of exceptional points is a codimension 2 manifold in state space. For example, in models of petroleum engineering [5, 19], exceptional points typically exist on the boundaries of elliptic regions.

Condition (4.1) implies that we cannot apply the implicit function theorem for solving the equation $\Phi(\xi, e, \varepsilon, u) = 0$ with respect to e and ξ. The standard way to study solutions of such an equation is provided by singularity theory, see [11]. It consists of (i) Liapunov–Schmidt reduction of the system $\Phi(\xi, e, \varepsilon, u) = 0$ to a single scalar equation $g(\eta, \varepsilon, u) = 0$ (with a one-to-one correspondence between the solutions $\xi(\varepsilon, u)$, $e(\varepsilon, u)$ and $\eta(\varepsilon, u)$), (ii) analysis of the reduced scalar equation, and (iii) interpretation of the results in terms of the original system variables.

In this section, we will use the direction vector e normalized as

$$(e - r_0) \cdot r_0 = 0 \tag{4.2}$$

instead of the condition $\|e\| = 1$ used above. The reason is that condition (4.2) facilitates the Liapunov–Schmidt reduction.

4.1. *Liapunov–Schmidt reduction*

Theorem 4.1. *For the exceptional point U_0 at the elliptic boundary, Eq.* (3.7) *can be solved for ξ and e in the neighborhood of $(\xi, e, \varepsilon, u) = (0, r_0, 0, 0)$ in the form*

$$e(\varepsilon, u) = r_0 - \frac{1}{2} G d^2F(r_0, r_0)\xi + r_1\varepsilon - GEd^2F(u, r_0) + o(\varepsilon, \|u\|), \tag{4.3}$$

where $\xi(\varepsilon, u)$ is a solution of the scalar equation

$$\alpha_0\xi^2 + \alpha_1\xi\varepsilon - \varepsilon^2 + n\cdot u + g_{\xi u}u\xi + 2q\cdot u\varepsilon + \frac{1}{2}\,g_{uu}(u,u) + o(\xi^2,\varepsilon^2,\|u\|^2) = 0 \tag{4.4}$$

with coefficients

$$\begin{aligned}
\alpha_0 &= \frac{1}{6}\,l_0 d^3F(r_0,r_0,r_0) - \frac{1}{2}\,n\cdot Gd^2F(r_0,r_0),\\
\alpha_1 &= \frac{1}{2}\,n\cdot r_1 + q\cdot r_0,\\
g_{\xi u}u &= \frac{1}{2}\,l_0 d^3F(u,r_0,r_0) - \frac{1}{2}\,l_0 d^2F(u, Gd^2F(r_0,r_0))\\
&\quad - l_0 d^2F(r_0, GEd^2F(u,r_0)),\\
g_{uu}(u,u) &= l_0 d^3F(u,u,r_0) - 2l_0 d^2F(u, GEd^2F(u,r_0)).
\end{aligned} \tag{4.5}$$

The matrix G is given in (3.15)*, and E the matrix $E = I - r_1 l_0$.*

Proof. Let us introduce the vector $y = \begin{pmatrix}\xi\\ h\end{pmatrix} \in \mathbb{R}^{m+1}$, where $h = e - r_0$. According to (4.2),

$$h\cdot r_0 = 0. \tag{4.6}$$

Then we can write the equation $\Phi(\xi, e, \varepsilon, u) = 0$ as $\Phi(y, \varepsilon, u) = 0$ (keeping the same letter is not confusing as the number and type of the arguments is different). The $(m+1)$-dimensional vector y belongs to the m-dimensional subspace defined by (4.6); also, $y = 0$ when $\xi = 0$ and $e = r_0$. Using (3.16), we find the following formulae for the derivatives of $\Phi(y, \varepsilon, u)$ at $(y, \varepsilon, u) = (0, 0, 0)$:

$$\begin{gathered}
L\,dy \equiv \Phi_y dy = \frac{1}{2}\,d^2F(r_0,r_0)\,d\xi + (A_0 - \sigma_0 I)\,dh,\\
\Phi_{yy}(dy_1, dy_2) = d^2F(dh_2, r_0)d\xi_1 + d^2F(dh_1, r_0)d\xi_2 + \frac{1}{3}\,d^3F(r_0,r_0,r_0)\,d\xi_1 d\xi_2,\\
\Phi_u du = d^2F(du, r_0), \quad \Phi_{uu}(du,du) = d^3F(du,du,r_0),\\
\Phi_{yu}(dy, du) = \frac{1}{2}\,d^3F(du,r_0,r_0)d\xi + d^2F(du, dh),\\
\Phi_\varepsilon = -r_0, \quad \Phi_{y\varepsilon}dy = -dh, \quad \Phi_{u\varepsilon} = 0, \quad \Phi_{\varepsilon\varepsilon} = 0.
\end{gathered} \tag{4.7}$$

Here subscripts denote derivatives with respect to the corresponding variable.

The linear operator L has one-dimensional null-space for vectors y satisfying condition (4.6). It is easy to see that the vector $v_0 \in \ker L$ can be taken as

$$v_0 = \begin{pmatrix} 1 \\ -\dfrac{1}{2}Gd^2F(r_0,r_0) \end{pmatrix}, \tag{4.8}$$

where the matrix G is defined in (3.15). Indeed, by using the degeneracy condition (3.9), (4.1) and the last equality in (3.21), one can check that the vector $-\frac{1}{2}Gd^2F(r_0,r_0)$ is orthogonal to r_0, i.e. condition (4.6) is satisfied. Thus, using (4.6) and (4.7),

$$Lv_0 = \frac{1}{2}\,d^2F(r_0,r_0) + G^{-1}\left(-\frac{1}{2}\,Gd^2F(r_0,r_0)\right) = 0. \tag{4.9}$$

The left null-space of L is given by the left eigenvector l_0, so that $l_0L = 0$. The matrix $E = I - r_1l_0$ defines the projection operator from $\mathbb{R}^n$ onto range L; this property follows from relations (3.4) and (3.5). Finally, we define the inverse operator L^{-1} on range L as

$$L^{-1}a \equiv \begin{pmatrix} 0 \\ Ga \end{pmatrix}. \tag{4.10}$$

According to the Liapunov–Schmidt reduction procedure, the solution of equation $\Phi(y,\varepsilon,u)$ in the neighborhood of $(0,0,0)$ can be given as

$$y = \eta v_0 + W(\eta,\varepsilon,u), \tag{4.11}$$

where η is a solution of a scalar equation $g(\eta,\varepsilon,u) = 0$, and W belongs to range L^{-1}, i.e. its first component is zero. The first component of relation (4.11) yields $\xi = \eta$. The smooth functions $g(\eta,\varepsilon,u)$ and $W(\eta,\varepsilon,u)$ can be found as a Taylor expansion. Their derivatives taken at $(0,0,0)$ are given by the formulae [11, Chap. 1]:

$$\begin{gathered} g_\eta = 0, \quad g_{\eta\eta} = l_0\Phi_{yy}(v_0,v_0), \quad g_\alpha = l_0\Phi_\alpha, \quad g_{\eta\alpha} = l_0\Phi_{y\alpha}v_0 + l_0\Phi_{yy}(v_0,W_\alpha), \\ g_{\alpha\alpha} = l_0\Phi_{\alpha\alpha} + 2l_0\Phi_{y\alpha}W_\alpha + l_0\Phi_{yy}(W_\alpha,W_\alpha), \quad W_\eta = 0, \quad W_\alpha = -L^{-1}E\Phi_\alpha, \end{gathered} \tag{4.12}$$

where subscripts denote derivatives with respect to the corresponding variables, and α stands for ε or u. By using (4.7), (4.8), (4.10) in (4.12), we find

$$\begin{gathered} g_\eta = 0, \quad g_{\eta\eta} = \frac{1}{3}\,l_0d^3F(r_0,r_0,r_0) - n\cdot Gd^2F(r_0,r_0), \\ g_\varepsilon = 0, \quad g_{\varepsilon\varepsilon} = -2, \quad g_{\eta\varepsilon} = \frac{1}{2}\,n\cdot r_1 + q\cdot r_0, \quad g_u du = n\cdot du, \quad g_{u\varepsilon}du = 2q\cdot du, \\ g_{\eta u}du = \frac{1}{2}\,l_0d^3F(du,r_0,r_0) - \frac{1}{2}\,l_0d^2F(du,Gd^2F(r_0,r_0)) \\ - l_0d^2F(r_0,GEd^2F(du,r_0)), \\ g_{uu}(du,du) = l_0d^3F(du,du,r_0) - 2l_0d^2F(du,GEd^2F(du,r_0)), \\ W_\eta = 0, \quad W_\varepsilon = \begin{pmatrix} 0 \\ r_1 \end{pmatrix}, \quad W_u du = \begin{pmatrix} 0 \\ -GEd^2F(du,r_0) \end{pmatrix}. \end{gathered} \tag{4.13}$$

Here we also used (3.4), (3.5), (3.9), (3.21) and the relations $GEr_0 = Gr_0 = r_1$, $l_0GE = l_1E = l_1$. Then the expressions in the theorem follow directly from (4.11) and (4.13). □

4.2. *Singularities of Hugoniot curves*

Let us consider Eq. (4.4) for left states $U_- = U_0 + u$ such that $n \cdot u \sim \|u\|$. Formally, this corresponds to perturbations u along a line passing through U_0 transversal to the elliptic boundary (the other situation, when $n \cdot u \ll \|u\|$, will be considered later). In the case $n \cdot u \sim \|u\|$, we can neglect higher order terms (the terms in the second row) in (4.4) to obtain the following asymptotic equation

$$\alpha_0 \xi^2 + \alpha_1 \xi \varepsilon - \varepsilon^2 + n \cdot u = 0. \tag{4.14}$$

This equation defines a curve in the (ε, ξ)-plane. If $n \cdot u > 0$, this curve intersects the ε-axis at the points

$$\xi = 0, \quad \varepsilon = \pm\sqrt{n \cdot u}. \tag{4.15}$$

Remark that Eq. (4.14) with $u = 0$ corresponds to the normal form $\xi^2 \pm \varepsilon^2 = 0$ whose universal unfolding is $\xi^2 \pm \varepsilon^2 + \alpha = 0$, see [11]. This means that Eq. (4.14) describes the generic unfolding of a singularity in the neighborhood of $(\xi, \varepsilon, u) = (0, 0, 0)$.

Using asymptotic expression (4.3) in (3.6), the Hugoniot curve for $U_+ = U_0 + u + \xi e$ is given by

$$U_+ = U_0 + u + \xi \left(r_0 - \frac{1}{2} Gd^2F(r_0, r_0)\xi + r_1 \varepsilon \right), \tag{4.16}$$

where again we kept only the essential lowest order terms (according to (4.14), the geometry of the Hugoniot curve is described by ε in the interval $\varepsilon \lesssim \sqrt{\|u\|}$ and $\xi \sim \varepsilon$). The points with $\xi = 0$ in (4.15) correspond to the self-intersection point of the Hugoniot curve at $U_+ = U_- = U_0 + u$. Naturally, the self-intersection exists only for $n \cdot u > 0$, when U_- belongs to the hyperbolic region.

There are two cases distinguished by the sign of the quantity

$$D = \alpha_1^2 + 4\alpha_0. \tag{4.17}$$

If $D < 0$, then for $u = 0$ (i.e. for the left shock state at the exceptional point $U_- = U_0$), Eq. (4.14) has only the trivial solution $\xi = \varepsilon = 0$. For left states U_- lying in the hyperbolic region ($n \cdot u > 0$), the solution of (4.14) represents an ellipse in the (ε, ξ)-plane, see Fig. 2(a). This ellipse determines an eight-shaped curve in state space, see Fig. 2(b). According to (4.16), this curve is elongated in the direction of r_0, i.e. parallel to the elliptic boundary (recall that r_0 is tangent to the elliptic boundary at the exceptional point, see (4.1)). As $U_- \to U_0$ in the hyperbolic region, the eight-shaped Hugoniot curve shrinks to a point. For left states U_- lying in the elliptic region ($n \cdot u < 0$), Eq. (4.14) has no solutions, so the Hugoniot curve does not exist (at least locally).

For $D > 0$, the solution of (4.14) for $u = 0$ is given by two lines

$$\varepsilon = \left(\alpha_1 \pm \sqrt{D} \right) \xi/2 \tag{4.18}$$

intersecting at the origin, see Fig. 3(a). These lines determine two curves in state space passing through the exceptional point U_0 tangent to the elliptic boundary

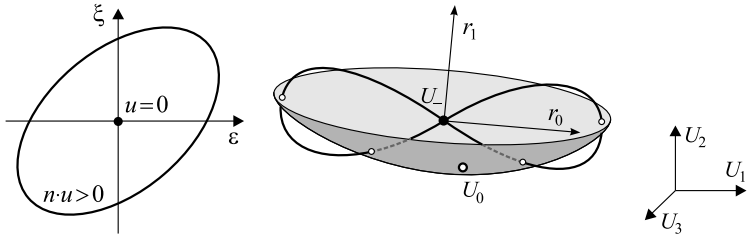

(a) (b)

Fig. 2. Hugoniot curves near the exceptional point for $D < 0$. The elliptic region lies below the gray surface.

along the eigenvector r_0, Fig. 3(b). A detailed analysis using inequality (4.25) below shows that either both curves lie in the hyperbolic region, or one curve lies in the hyperbolic region and the other in the elliptic region. Figure 3 corresponds to the case when both curves lie in the hyperbolic region. For left states U_- lying in the hyperbolic region ($n \cdot u > 0$), the solution of (4.14) is given by two branches of a hyperbola in the (ε, ξ)-plane lying in the left and right quadrants. In state space, these branches intersect at U_-, Fig. 3(c). Finally, for left states U_- lying in the elliptic region ($n \cdot u < 0$), the solution is given by two branches of a hyperbola lying in the upper and lower quadrants. Then there are two separated Hugoniot branches which do not pass through U_-, Fig. 3(d).

Now consider the case $n \cdot u \ll \|u\|$, when the left shock state is much closer to the elliptic boundary than to the exceptional point (this happens for perturbations u along a curve tangent to the elliptic boundary at U_0). We are interested in the situation when $n \cdot u \sim \|u\|^2$. In this case all terms in Eq. (4.4) are of the same order of magnitude. The solution of Eq. (4.4) in the (ε, ξ)-plane is an ellipse (or the empty set) if $D < 0$, and it is a hyperbola if $D > 0$. Unlike the previous case, these curves (ellipse or hyperbola) are not centered at the origin. The curves intersect the ε-axis for U_- in the hyperbolic region, they are tangent to the ε-axis for U_- at the elliptic boundary, and have no intersection with the ε-axis for U_- in the elliptic region. This follows from the result in classical theory that there are two transversal Hugoniot curves passing through U_- (recall that this corresponds to $\xi = 0$) for U_- in the hyperbolic region. In state space, the Hugoniot curves are described by the formula $U_+ = U_0 + u + \xi e$ with e given by expression (4.3). If the position of the ellipse or hyperbola relative to the ε-axis is the same as in Fig. 2(a) or 3(a), then the Hugoniot curves in state space have qualitatively the same form as described above. The other four possibilities, when the ellipse is tangent or does not intersect the ε-axis, and when the hyperbolae are tangent or intersect the ε-axis, are shown in Fig. 4. These cases represent transitions from singular structures of shock curves near exceptional points to regular structures described in Sec. 3.

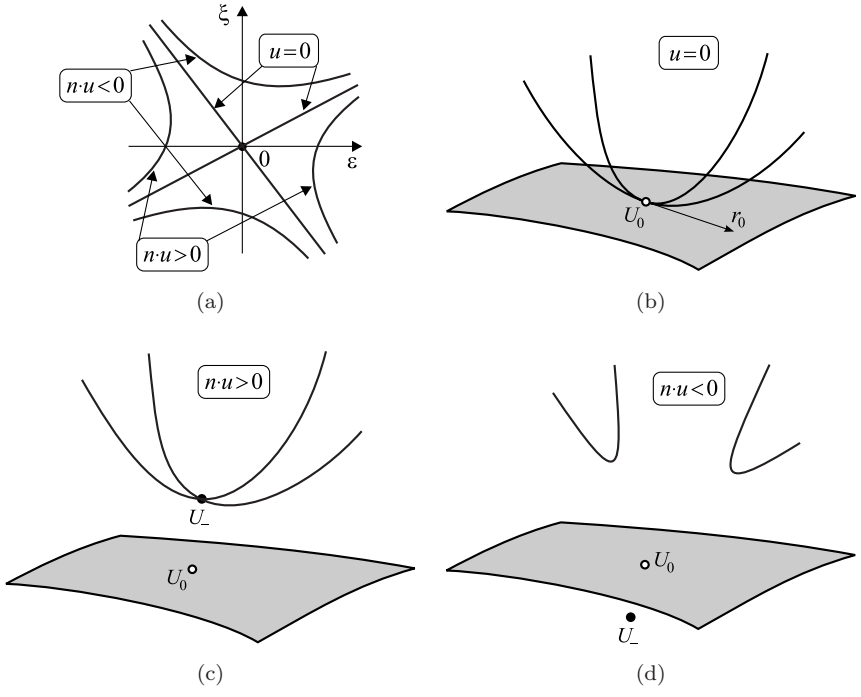

Fig. 3. Hugoniot curves near the exceptional point for $D > 0$. The elliptic region lies below the gray surface.

Remark 4.2. For a system of two conservation laws with a quadratic flux function, we have $r_0 = l_1^T$, $r_1 = l_0^T$ and $G = r_0 l_0 + r_1 l_1$. Then, at the exceptional point $(n \cdot r_0 = 0)$, we find

$$\alpha_0 = -\frac{1}{2}\, n \cdot G d^2 F(r_0, r_0) = -\frac{1}{2}\, (n \cdot r_1) l_1 d^2 F(r_0, r_0)$$
$$= -(n \cdot r_1) \left(q \cdot r_0 - \frac{1}{2}\, n \cdot r_1 \right). \tag{4.19}$$

Using α_1 from (4.5) yields

$$D = \alpha_1^2 + 4\alpha_0 = \left(q \cdot r_0 - \frac{3}{2}\, n \cdot r_1 \right)^2 \geq 0. \tag{4.20}$$

This proves that the singularity of type shown in Fig. 2 ($D < 0$) does not arise in systems of two conservation laws with quadratic flux functions.

4.3. *Admissible shocks*

Let us check the Lax conditions (2.3) along the Hugoniot curve. We consider the cases $n \cdot u \sim \|u\|$ shown in Figs. 2 and 3. (In this paper, we do not study the Lax

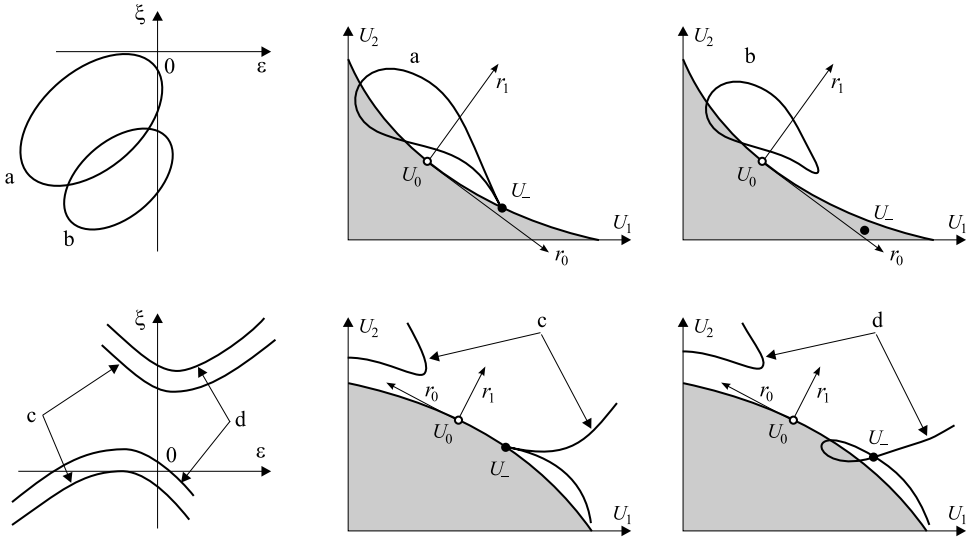

Fig. 4. Hugoniot curves near the exceptional point for $n \cdot u \sim \|u\|^2$ (the elliptic region is gray).

conditions in the case $n \cdot u \sim \|u\|^2$, which is more complicated.) Then, according to asymptotic equation (4.14), the following quantities have the same order of magnitude: $\varepsilon \sim \xi \sim \|u\|^{1/2}$. For the characteristic speeds $\lambda_{k,k+1}(U_-)$ with $U_- = U_0 + u$ we have the same asymptotic relation as in (3.27):

$$\lambda_{k,k+1}(U_-) = \sigma_0 \pm \sqrt{n \cdot u}, \tag{4.21}$$

which contains the terms of order $\|u\|^{1/2}$. The main correction term in expansion (4.16) for U_+ is $\Delta U_+ \approx \xi r_0 \sim \|u\|^{1/2}$. This term vanishes when we substitute (4.16) into (3.26), because $n \cdot r_0 = 0$. This means that the square root and the linear terms in (3.26) are of the same order $\sim \|u\|^{1/2}$. In order to find the asymptotic values for characteristic speeds, one must use the second order approximation for the expression inside the square root in (3.24) of the following form [24, Chap. 2]:

$$l_0 B r_0 + \frac{1}{4}\,(l_1 B r_0 + l_0 B r_1)^2 - l_0 B G B r_0 + o(\|B\|^2). \tag{4.22}$$

(This expression corresponds to a degenerate type of bifurcation of a double eigenvalue when $l_0 B r_0 \sim \|B\|^2$.) Using expansions (3.25) and (4.16) in (4.22) and substituting the result into (3.24), one finds the asymptotic expression

$$\lambda_{k,k+1}(U_+)$$
$$= \sigma_0 + q \cdot r_0 \xi \pm \sqrt{((q \cdot r_0)^2 + \frac{1}{2}\, l_0 d^3 F(r_0, r_0, r_0) - \frac{3}{2}\, n \cdot G d^2 F(r_0, r_0))\xi^2 + n \cdot r_1 \varepsilon \xi + n \cdot u}, \tag{4.23}$$

where we kept only the leading terms of order $\|u\|^{1/2}$. By using the quantities α_0, α_1 defined in (4.5) and Eq. (4.14), we write (4.23) as

$$\lambda_{k,k+1}(U_+) = \sigma_0 + q \cdot r_0\xi \pm \sqrt{(\varepsilon - q \cdot r_0\xi)^2 + \xi(\alpha_1\varepsilon + 2\alpha_0\xi)}. \tag{4.24}$$

The right state U_+ lies in the hyperbolic region if

$$(\varepsilon - q \cdot r_0\xi)^2 + \xi(\alpha_1\varepsilon + 2\alpha_0\xi) > 0. \tag{4.25}$$

First, consider the left states U_- in the hyperbolic region ($n \cdot u > 0$). Using (4.21) and (4.24) in (2.3) (with $\sigma = \sigma_0 + \varepsilon$), we write the admissibility conditions for the k-shock as

$$k\text{-shock: } \varepsilon < -\sqrt{n \cdot u}, \quad \xi(\alpha_1\varepsilon + 2\alpha_0\xi) > 0, \tag{4.26}$$

Comparing (4.25) and (4.26), it is easy to see that the right states U_+ of k-shocks lie in the hyperbolic region. Similarly, for $(k+1)$-shocks we find

$$(k+1)\text{-shock: } -\sqrt{n \cdot u} < \varepsilon < \sqrt{n \cdot u}, \quad \xi(\alpha_1\varepsilon + 2\alpha_0\xi) < 0, \quad \varepsilon > q \cdot r_0\xi. \tag{4.27}$$

Conditions (4.26) and (4.27) determine two segments in the Hugoniot curve with one end at U_- and, possibly, a separate segment for k and/or $(k+1)$-shocks.

Consider now the left states U_- in the elliptic region ($n \cdot u > 0$). Using (4.21) and (4.24) in (2.3), we write the admissibility conditions for the k-shock as

$$k\text{-shock: } \varepsilon < 0, \quad \xi(\alpha_1\varepsilon + 2\alpha_0\xi) > 0. \tag{4.28}$$

There are no $(k+1)$-shocks in this case.

We remark that by using formulae (4.21) and (4.24), one can find segments of Hugoniot curves satisfying shock speed conditions different from (2.3), e.g. the segments containing possible states of certain non-Lax shocks ($S_{i,j}$ shocks [17]).

5. Riemann Solutions with States in the Elliptic Region

Consider the Riemann problem for the system of conservation laws (2.1), i.e. the weak scale-invariant solution $U(x,t) = \tilde{U}(x/t)$ for piecewise constant initial data with a single jump at $x = 0$:

$$U(x,0) = \begin{cases} L, & x < 0; \\ R, & x > 0. \end{cases} \tag{5.1}$$

When both L and R are very near each other and both lie in the hyperbolic region, Riemann solutions are described by the standard Lax diagram [25]. For initial data near the elliptic boundary, Riemann solutions were discussed in [5, 7, 12, 21] for systems of two conservation laws. In this section, we contribute with an example of the Riemann solution for two conservation laws with left initial condition L in the elliptic region near the boundary, and right initial condition R in the hyperbolic region. This example illustrates the asymptotic description of Hugoniot curves given in Sec. 3.

A typical Riemann solution is a sequence of two waves (rarefactions and/or shocks) separated by a constant state M. Rarefaction waves are smooth solutions $U(\lambda)$ parametrized by the speed $\lambda = x/t$ satisfying the equation $A(U)U' = \lambda U'$, where $U' = dU/d\lambda$. The rarefaction wave defines a curve in state space, which is tangent at each point to one of the eigenvectors of the matrix $A(U)$. Given the left state U_- in the hyperbolic region, the rarefaction curve and the shock curve (the curve of right states for admissible shocks) lie at opposite sides of U_-, where they are tangent, see e.g. [25]. The structure of rarefaction curves near the elliptic boundary is described in [16].

Consider the left initial condition L in the elliptic region close to the boundary. Then the slower wave in the Riemann solution is a shock; its right state is the intermediate state of the Riemann solution M, see Fig. 5. The thick solid line in the figure shows possible states M for fixed L (this is the part of the Hugoniot curve for $U_- = L$ corresponding to admissible shocks satisfying (2.3); M_0 is the end point of this part corresponding to $\sigma = \operatorname{Re}\lambda_1(U_-)$). Figure 5 corresponds to L far away from any of exceptional points, see Fig. 1(c). The faster wave may be a shock or a rarefaction. Thus, there are two typical structures of Riemann solutions for different right initial conditions. The first Riemann solution consists of a shock S_1 (from L to M) followed by a shock S_2 (from M to R). These Riemann solutions correspond to R lying in the region marked S_1S_2 in Fig. 5. The second Riemann solution consists of a shock S_1 (from L to M) followed by a rarefaction of the second characteristic family $\mathcal{R}_2$ (from M to R). These Riemann solutions correspond to R lying in the region marked $S_1\mathcal{R}_2$ in Fig. 5. Local Riemann solutions with the right states R to the right of the thick dashed line do not exist. This line consists of the rarefaction curve $\mathcal{R}_2$ from M_0 (the part of the curve to the right of M_0 in Fig. 5) and right states of S_2 shocks from M_0 (the part of the curve to the left of M_0 in Fig. 5).

Consider the Riemann problem for system (2.1) with flux function and initial conditions

$$F(U) = \begin{pmatrix} (U_2)^2 \\ U_1 \end{pmatrix}, \quad L = \begin{pmatrix} 0 \\ -0.02 \end{pmatrix}, \quad R = \begin{pmatrix} 0.02 \\ 0.16 \end{pmatrix}. \tag{5.2}$$

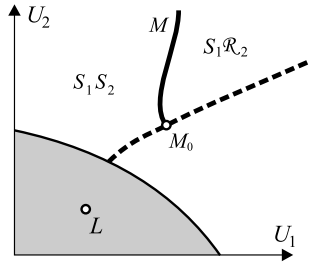

Fig. 5. Diagram of possible right initial states R in Riemann solutions for a left initial state L in the elliptic region.

The characteristic speeds at $U = (U_1, U_2)$ are $\lambda_1 = -\sqrt{2U_2}$ and $\lambda_2 = \sqrt{2U_2}$. The elliptic region is the lower half-plane $U_2 < 0$, so L is in the elliptic region, and R is in the hyperbolic region. For the left state $U_- = L$, we find all possible right states U_+ from the Rankine–Hugoniot equation (2.2) as

$$U_+ = \begin{pmatrix} \sigma(0.04 + \sigma^2) \\ 0.02 + \sigma^2 \end{pmatrix}. \tag{5.3}$$

By checking the admissibility conditions (2.3), we find that 1-shocks correspond to $\sigma < 0$ (the value $\sigma = 0$ corresponds to the end point $M_0 = (0,\ 0.02)$, see Fig. 5). This can be compared with the asymptotic expression (3.23) evaluated for the elliptic boundary point $U_0 = (0,\ 0)$. At this point $\sigma_0 = 0$, and we find

$$\begin{gathered} r_0 = \begin{pmatrix} 0 \\ 1 \end{pmatrix}, \quad r_1 = \begin{pmatrix} 1 \\ 0 \end{pmatrix}, \quad l_0 = (1,\ 0), \quad l_1 = (0,\ 1), \\ u = \begin{pmatrix} 0 \\ -0.02 \end{pmatrix}, \quad n = \begin{pmatrix} 0 \\ 2 \end{pmatrix}. \end{gathered} \tag{5.4}$$

Substituting (5.4) into (3.23) gives the exact expression (5.3).

By solving the equation $A(U)U' = \lambda U'$ for the rarefaction of the second family ($\lambda = \lambda_2 = \sqrt{2U_2}$) with the right state R given in (5.2), we obtain the states on the rarefaction wave as

$$U(\lambda) = \begin{pmatrix} 0.02 + \left(\lambda^3 - 0.128\sqrt{2}\right)/3 \\ \lambda^2/2 \end{pmatrix}. \tag{5.5}$$

The right state of the shock (5.3) must be equal to the left state of the rarefaction (5.5). Numerical computation yields the intermediate state and shock speed as

$$\sigma = -0.2311, \quad M = \begin{pmatrix} -0.02158 \\ 0.07340 \end{pmatrix}. \tag{5.6}$$

The shock is admissible since $\sigma < 0$. Thus, we found the Riemann solution with one shock and one rarefaction wave. The shock has the speed and right state (5.6), and the rarefaction is given by (5.5) with $0.3831 \le \lambda \le 0.4\sqrt{2}$.

Numerical simulations were carried out using a linearized Crank–Nicolson scheme for two viscous conservation laws (2.4) with coefficient $\epsilon = 0.01$ of the parabolic term and data (5.2). Figure 6 shows the numerical solution in (U_1, U_2), (x, U_1) and (x, U_2) spaces at a certain time. This solution represents a traveling wave S_1 from L to M, which becomes a shock as $\epsilon \to +0$, followed by a rarefaction wave $\mathcal{R}_2$ from M to R. The numerical solution agrees very well with the analytic Riemann solution (5.3), (5.5), (5.6). We also observed stability of this solution.

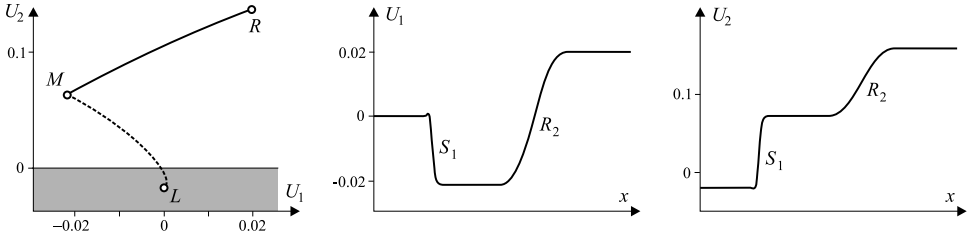

Fig. 6. Numerical simulations of the Riemann solution with one shock and rarefaction wave (the elliptic region is gray).

6. Discussion

The Lax diagram for the structure of the Riemann solution changes for elliptic left states near regular points of the elliptic boundary. Shock-shock and shock-rarefaction sequences are preserved, but there are no local solutions in half a region near the left state, out of the elliptic region, because there are no rarefaction waves emanating from this left state. This gap may be filled by non-local solutions.

The structure of the Riemann solution near exceptional points of the elliptic boundary is very rich, as already shown in our analysis of the Hugoniot curves that parametrize shocks. To understand it, it is necessary to study the traveling waves for these shocks. An initial step using the results of [8] on bifurcations of planar vector fields was taken in [4], where quadratic flux functions were studied. A program for finding Riemann solutions for nonhomogeneous quadratic flux functions under the viscous profile condition for shocks was initiated in [2], and continued in [20], where two examples were solved, and theoretically in [9]. Our work shows that cubic terms in the flux function must be considered. Remark that the effect of the cubic terms vanishes as the elliptic region shrinks to a point. At this point, a double semi-simple eigenvalue (characteristic speed) appears, and the statement can be proved by analyzing local behavior of eigenvalues and eigenvectors [24].

Acknowledgments

This work was supported by CNPq under Grants 301532/2003-6, 300097/2004-2, 304168/2006-8, 472067/2006-0, 300668/2007-4, FAPERJ under Grant E-26/152.163/2002, E-26/152.525/2006, E-26/110.310/2007, CAPES under Grant 0722/2003 (PAEP no. 0143/03-00), FINEP under Grant 01.02.0212.00 and President of Russian Federation Grant No. MK-2012.2006.1.

References

[1] V. I. Arnold, *Geometrical Methods in the Theory of Ordinary Differential Equations* (Springer, New York, 1983).

[2] A. V. Azevedo, Multiple fundamental solutions for hyperbolic-elliptic systems of conservation laws, Ph.D. thesis, PUC-RIO, Rio de Janeiro (1991).
[3] A. V. Azevedo and D. Marchesin, Multiple viscous profile Riemann solutions in mixed elliptic-hyperbolic models for flow in porous media, in *Nonlinear Evolution Equations that Change Type*, The IMA Volumes in Mathematics and Its Applications, Vol. 27 (Springer, New York, 1990), pp. 1–17.
[4] A. V. Azevedo, D. Marchesin, B. Plohr and K. Zumbrun, Capillary instability in models for three-phase flow, *Z. Angew. Math. Phys.* **53** (2002) 713–746.
[5] J. B. Bell, J. A. Trangenstein and G. R. Shubin, Conservation laws of mixed type describing three-phase flow in porous media, *SIAM J. Appl. Math.* **46** (1986) 1000–1017.
[6] S. Canic, Nonexistence of Riemann solutions for a quadratic model deriving from petroleum engineering, *Nonlinear Anal. Real World Appl.* **4** (2003) 373–408.
[7] S. Canic, B. L. Keyfitz and E. H. Kim, Mixed hyperbolic-elliptic systems in self-similar flows, *Bol. Soc. Brasil. Mat.* **32** (2002) 1–23.
[8] F. Dumortier, R. Roussarie and J. Sotomayor, *Bifurcation of Planar Vector Fields*, Lecture Notes in Mathematics, Vol. 1480 (Springer, Berlin, 1991).
[9] C. Eschenazi and C. F. Palmeira, Local topology of elementary waves for systems of two conservation laws, *Mat. Contemp.* **15** (1998) 127–144.
[10] H. Frid, Measure-valued solutions for multiphase flow in porous media, *J. Math. Anal. Appl.* **196** (1995) 614–627.
[11] M. Golubitsky and D. G. Schaeffer, *Singularities and Groups in Bifurcation Theory* (Springer, New York, 1985).
[12] H. Holden, On the Riemann problem for a prototype of a mixed type conservation law, *Commun. Pure Appl. Math.* **40** (1987) 229–264.
[13] E. L. Isaacson, D. Marchesin, C. F. Palmeira and B. J. Plohr, A global formalism for nonlinear waves in conservation laws, *Commun. Math. Phys.* **146** (1992) 505–552.
[14] B. L. Keyfitz, A geometric theory of conservation laws which change type, *Z. Angew. Math. Mech.* **75** (1995) 571–581.
[15] B. L. Keyfitz, R. Sanders and M. Sever, Lack of hyperbolicity in the two-fluid model for two-phase incompressible flow, *Discrete Contin. Dynam. Syst. Ser. B* **3** (2003) 541–563.
[16] A. A. Mailybaev and D. Marchesin, Hyperbolicity singularities in rarefaction waves, to appear in *J. Dynam. Differential Equations* **20** (2008) 1–29.
[17] A. A. Mailybaev and D. Marchesin, Dual-family viscous shock waves in n conservation laws with application to multi-phase flow in porous media, *Arch. Ration. Mech. Anal.* **182** (2006) 1–24.
[18] D. Marchesin and C. F. B. Palmeira, Topology of elementary waves for mixed-type systems of conservation laws, *J. Dynam. Differential Equations* **6** (1994) 427–446.
[19] D. Marchesin and B. Plohr, Wave structure in WAG recovery, *Soc. Petroleum Eng. J.* **6** (2001) 209–219.
[20] V. M. M. Matos, Riemann problem for two conservation laws of type IV with elliptic region, Ph.D. thesis, IMPA, Rio de Janeiro (2004) (in Portuguese).
[21] V. Matos and D. Marchesin, High amplitude solutions for small data in pairs of conservation laws that change type, in *Hyperbolic Problems: Theory, Numerics, Applications* (Springer, Berlin, 2008), pp. 711–719.
[22] H. B. Medeiros, Stable hyperbolic singularities for three-phase flow models in oil reservoir simulation, *Acta Appl. Math.* **28** (1992) 135–159.

[23] W. Schulte and A. Falls, Features of three-component, three-phase displacement in porous media, *SPE Reservoir Eng.* **7** (1992) 426–432.
[24] A. P. Seyranian and A. A. Mailybaev, *Multiparameter Stability Theory with Mechanical Applications* (World Scientific, Singapore, 2003).
[25] J. Smoller, *Shock Waves and Reaction-Diffusion Equations* (Springer, New York, 1983).